Hydroelastic theory for offshore floating plates of variable flexural rigidity

S. Michele[a], S. Zheng[b,a] , E. Renzi[c], A.G.L. Borthwick[b], D.M. Greaves[b]
a. School of Engineering, Computing and Mathematics, University of Plymouth, UK
b. Ocean College, Zhejiang University, Zhoushan 316021, Zhejiang, China
c. Mathematics of Complex and Nonlinear Phenomena, Department of Mathematics, Physics and Electrical Engineering, Northumbria University, UK
Email: simone.michele@plymouth.ac.uk

1 Introduction

We present a theoretical model of the hydrodynamic behaviour of a floating flexible plate of variable flexural rigidity connected to the seabed by a spring/damper system. Decomposition of the response modes into rigid and bending elastic components allows us to investigate the hydroelastic behaviour of the plate subject to monochromatic incident free-surface waves. We show that spatially dependent plate stiffness affects the eigenfrequencies and modal shapes, with direct consequences on plate dynamics and wave power extraction efficiency.

2 Mathematical model

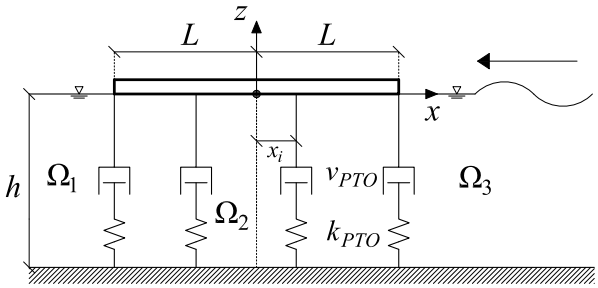

Figure 1: Side view of floating flexible plate. Vertical cables are located at points $x_i, i = 1, ..., \mathcal{I}$.

Figure 1 depicts a two–dimensional floating elastic plate of length $2L$ in open sea of constant depth h. A Cartesian reference system is defined with x-axis coincident with the undisturbed free-surface level and z-axis pointing vertically upward from still water level. The plate is connected to the seabed through vertical cables located at $x = x_i$, $i = 1, ..., \mathcal{I}$. Each cable has constant stiffness, k_{PTO}, and damping coefficient, ν_{PTO}. The system may be treated as continuous when there are large numbers of discrete cables present. We assume the thin-plate approximation, in which case the elastic vibration of the floater can be described by

$$\partial_{xx}\left(D\partial_{xx}W\right) = q - \mu\partial_{tt}W, \quad x \in [-L, L], \tag{1}$$

where W is the plate vertical displacement, t denotes time, q is the transverse distributed load (positive in the z-direction), $D(x)$ is the spatially dependent flexural rigidity, and μ is the constant mass per unit length of the plate. In defining the linearised hydrodynamic problem, inviscid fluid and irrotational flow are assumed, such that the velocity potential $\Phi(x, z, t)$ satisfies Laplace's equation in the fluid domain $\Omega = \Omega_1 \cup \Omega_2 \cup \Omega_3$ (see Figure 1). At the free surface, we apply the following kinematic and mixed boundary conditions,

$$\partial_t\zeta = \partial_z\Phi, \quad \partial_{tt}\Phi + g\partial_z\Phi = 0, \quad z = 0, \ |x| > L, \tag{2}$$

where ζ is free-surface elevation and g is acceleration due to gravity. In addition, we require the fluid velocity to be tangential to the seabed and

$$\partial_z\Phi = \partial_t W, \quad z = 0, \ x \in [-L, L]. \tag{3}$$

Let us assume the plate to be forced by monochromatic incident waves of frequency ω, hence $\{\Phi, \zeta, W\} = \mathrm{Re}\left\{(\phi, \eta, w)e^{-\mathrm{i}\omega t}\right\}$, in which i is the imaginary unit and variables have spatial dependence. We further decompose w into a set of rigid (heave w_h and pitch w_p) and elastic dry bending modes w_l (Newman 1994). Hence, $w = \zeta_h w_h + \zeta_p w_p + \sum_{l=0}^{\infty} \zeta_l w_l$. For simplicity we assume the spatial dependence $D = \sum_{m=1}^{M} D_m H[x - x_{m-1}]H[x_m - x]$ where H is the Heaviside step function, D_m is constant flexural rigidity along the mth plate segment, M is the total number of plate segments, and $x_0 = -L$ and $x_M = L$ define the edges of the plate. The general solution in each segment is readily given by

$$w_{lm} = a_{lm}\sinh\left[\sqrt{\omega_l}\beta_m x\right] + b_{lm}\cosh\left[\sqrt{\omega_l}\beta_m x\right] + c_{lm}\sin\left[\sqrt{\omega_l}\beta_m x\right] + d_{lm}\cos\left[\sqrt{\omega_l}\beta_m x\right], \quad (4)$$

where $\beta_m = (\mu/D_m)^{1/4}$. Usage of free-edge conditions and matching between each plate segment, yields a homogeneous system in terms of real constants a_{lm}, b_{lm}, c_{lm} and d_{lm}. Having completed the dry-beam modal analysis we are now in a position to solve the hydrodynamic problem. The velocity potential ϕ is expanded in diffraction and radiation components giving

$$\phi = \phi_D + \phi_R, \quad \phi_R = \zeta_h\phi_h + \zeta_p\phi_p + \sum_{l=0}^{\infty}\zeta_l\phi_l, \quad \phi_D = -\frac{\mathrm{i}Ag}{\omega}\frac{\cosh[k_0\,(h+z)]}{\cosh(k_0 h)}\mathrm{e}^{-\mathrm{i}k_0 x} + \phi_S, \quad (5)$$

where A is wave amplitude, k_0 satisfies the dispersion relation $\omega^2 = gk_0\tanh(k_0 h)$, ϕ_S is scattering velocity potential, ϕ_D is diffraction velocity potential, ϕ_R is radiation velocity potential, ϕ_h is heaving velocity potential, ϕ_p is pitching velocity potential, and ϕ_l is the radiation velocity potential related to the lth bending mode. Let $\phi^{(2)}$ be the velocity potential in the fluid subdomain below the plate Ω_2, $\phi^{(1)}$ be the velocity potential in the external subdomain Ω_1, and $\phi^{(3)}$ be the velocity potential in Ω_3. The general solution for each velocity potential reads

$$\phi^{(3)}_{D,\alpha} = \mathcal{A}_0^{D,\alpha}e^{\mathrm{i}k_0 x}\cosh[k_0\,(h+z)] + \sum_{j=1}^{\infty}\mathcal{A}_j^{D,\alpha}e^{-k_j x}\cos[k_j\,(h+z)], \quad (6)$$

$$\phi^{(1)}_{D,\alpha} = \mathcal{B}_0^{D,\alpha}e^{-\mathrm{i}k_j x}\cosh[k_0\,(h+z)] + \sum_{j=1}^{\infty}\mathcal{B}_j^{D,\alpha}e^{k_j x}\cos[k_j\,(h+z)], \quad (7)$$

$$\phi^{(2)}_{D} = \mathcal{C}_0^{D} + \mathcal{D}_0^{D}x + \sum_{j=1}^{\infty}\cos\left(\frac{j\pi z}{h}\right)\left[\mathcal{C}_j^{D}\cosh\left(\frac{j\pi x}{h}\right) + \mathcal{D}_j^{D}\sinh\left(\frac{j\pi x}{h}\right)\right], \quad (8)$$

$$\phi^{(2)}_{\alpha} = \tilde{\phi}_\alpha + \mathcal{C}_{\alpha 0}^{\alpha} + \mathcal{D}_{\alpha 0}^{\alpha}x + \sum_{j=1}^{\infty}\cos\left(\frac{j\pi z}{h}\right)\left[\mathcal{C}_{\alpha j}^{\alpha}\cosh\left(\frac{j\pi x}{h}\right) + \mathcal{D}_{\alpha j}^{\alpha}\sinh\left(\frac{j\pi x}{h}\right)\right] \quad (9)$$

where $\mathcal{A}_j^{D,\alpha}$, $\mathcal{B}_j^{D,\alpha}$, $\mathcal{C}_j^{D,\alpha}$ and $\mathcal{D}_j^{D,\alpha}$ are unknown complex constants determined by applying a eigenfunction expansion approach, k_j is the jth root of $\omega^2 = -gk_j\tan(k_j h)$, $j = 1, \ldots, \infty$, α refers to the heave mode, pitching mode, or lth bending elastic mode and $\tilde{\phi}_\alpha$ is a particular solution that accounts for the plate vibration. The particular solution for the rigid modes are

$$\tilde{\phi}_h = -\frac{\mathrm{i}\omega}{2h}\left[z^2 - x^2 + 2zh\right], \quad \tilde{\phi}_p = \frac{\mathrm{i}\omega x}{6h}\left[x^2 - 3z^2 - 6zh\right]. \quad (10)$$

It is challenging to find a suitable particular solution for $\tilde{\phi}_l$ that satisfies the boundary condition for each one of the bending modes, $\partial_z\tilde{\phi}_l = -\mathrm{i}\omega w_l$. Here we propose a simple approach based on Fourier sine series expansion of natural shapes. This procedure enables the particular velocity potential solution to remain continuous throughout the entire subdomain Ω_2 without requiring matching below the plate of stepped rigidity. Thus we assume

$$w_l(x) = \frac{w_l|_{x=L} + w_l|_{x=-L}}{2} + x\frac{w_l|_{x=L} - w_l|_{x=L}}{2L} + f_l(x), \quad (11)$$

where the first two terms in (11) represent constant and linear components, and the last term represents a deformed shape with zero displacement and nonzero derivative in $x = \pm L$. This decomposition enables us to write f_l in the form

$$f_l = \sum_{n=1}^{\infty} a_{nl} \sin\left[\frac{n\pi(x+L)}{2L}\right], \quad a_{nl} = \frac{1}{L}\int_{-L}^{L} f_l \sin\left[\frac{n\pi(x+L)}{2L}\right] \mathrm{d}x. \tag{12}$$

Using separation of variables method, the corresponding velocity potential is given by

$$\tilde{\phi}_l = \tilde{\phi}_h \frac{w_l|_{x=L} + w_l|_{x=-L}}{2} + \tilde{\phi}_p \frac{w_l|_{x=L} - w_l|_{x=L}}{2L} - \frac{2\mathrm{i}L\omega}{\pi} \sum_{n=0}^{\infty} \frac{a_{nl}}{n} \sin\left[\frac{n\pi(x+L)}{2L}\right] \frac{\cosh\left[\frac{n\pi(h+z)}{2L}\right]}{\sinh\left[\frac{n\pi h}{2L}\right]}.$$

The foregoing method is completely general and can be extended to any free surface deformation provided it can be expanded in the form (11). The dynamic equation (1) in presence of all external forces becomes after some manipulation

$$w\left[\rho g - \mu\omega^2 + \sum_{i=1}^{\mathcal{I}} \left(-\mathrm{i}\omega\nu_{PTO} + k_{PTO}\right)\delta\left(x - x_i\right)\right] + \sum_{l=0}^{\infty} \mu\omega_l w_l - \mathrm{i}\omega\rho\left(\phi_R^{(2)} + \phi_D^{(2)}\right) = 0. \tag{13}$$

where ρ is fluid density and δ denotes the Dirac Delta function. The complex modal amplitudes ζ_h, ζ_p and ζ_l are found by multiplying both sides of (13) by each of the modal shape functions w_α and then integrating over the wetted surface of the plate $x \in [-L, L]$. The average power generated by the plate is readily given by

$$P = \frac{1}{2}\nu_{PTO}\omega^2 \sum_{i=1}^{\mathcal{I}} \left| w_h\zeta_h + w_p\zeta_p + \sum_{l=0}^{\infty} w_l\zeta_l \right|_{x=x_i}^2, \tag{14}$$

hence the system efficiency is given by the capture-width ratio C_W

$$C_W = \frac{P}{\frac{1}{2}\rho g A^2 C_g}, \quad C_g = \frac{\omega}{2k_0}\left[1 + \frac{2k_0 h}{\sinh\left(2k_0 h\right)}\right], \tag{15}$$

where C_g is group celerity. The Haskind–Hanaoka formula valid for two-dimensional domains can be used to check numerical computations of diffraction and radiation velocity potentials. Its expression reads

$$F_\alpha = -2\mathrm{i}\rho g C_g A A_\alpha^+ \omega^{-1}, \quad A_\alpha^+ = \mathrm{i}\omega\cosh(k_0 h)\mathcal{A}_0^\alpha g^{-1}, \tag{16}$$

where F_α represents the exciting force, A_α is the Kochin function and $\mathcal{A}_0^\alpha$ is the first complex coefficient of the radiation potential. From (16) we can derive the most general expression for the capture-width ratio C_W expressed in terms of radiation velocity potentials

$$C_W = \mathrm{Re}\left\{2\sum_{\alpha=1}^{\infty} A_\alpha^+\zeta_\alpha^* - \sum_{\alpha=1}^{\infty}\sum_{\beta=1}^{\infty} \zeta_\alpha\zeta_\beta^*\left(A_\alpha^+ A_\beta^{+*} + A_\alpha^- A_\beta^{-*}\right)\right\}. \tag{17}$$

If plate motion is characterised by one symmetric or anti-symmetric mode, we obtain the well-known maximum value $C_W = 0.5$. Let us now consider two modes $\alpha = 1, 2$, one symmetric and the other anti-symmetric. Expression (17) becomes $C_W = 2\mathrm{Re}\left\{\sum_{\alpha=1}^{2} A_\alpha^+\zeta_\alpha^*\right\} - 2\sum_{\alpha=1}^{2}\left|\zeta_\alpha A_\alpha^+\right|^2$, which gives a theoretical upper bound $C_W = 1$ for $\mathrm{Re}\left\{A_1^+\zeta_1^*\right\} = \left|\zeta_1 A_1^+\right| = \mathrm{Re}\left\{A_2^+\zeta_2^*\right\} = \left|\zeta_2 A_1^+\right| = 1/2$, independent of plate size. However, the flexible floater considered herein also includes rigid and infinite bending elastic mode. This implies that multiple objective optimisation may lead to increased efficiency with respect to standard rigid WECs.

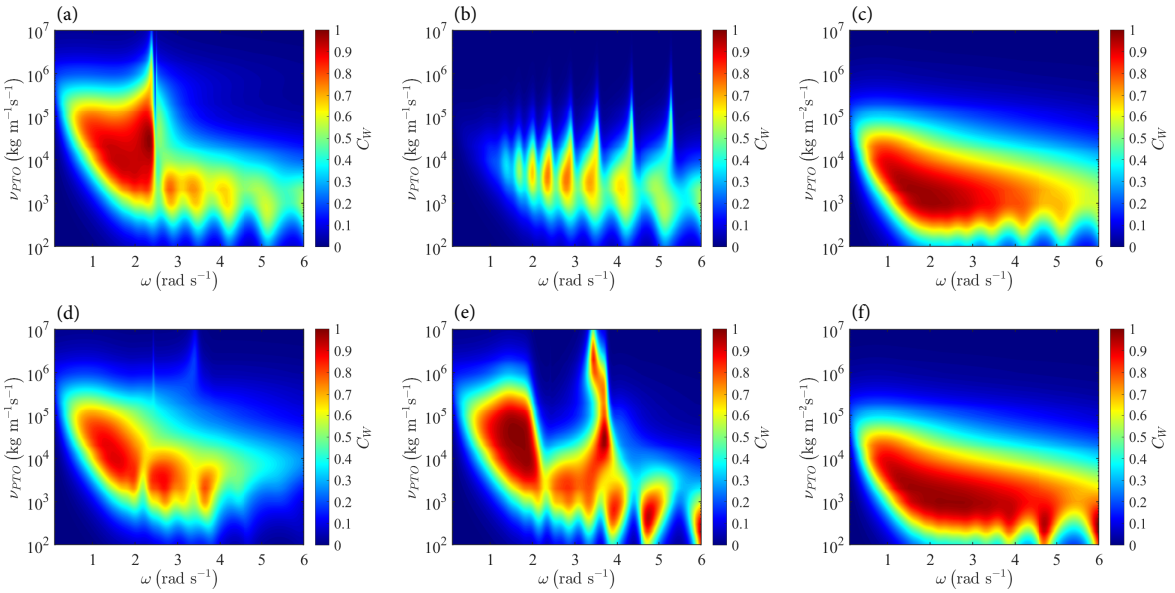

Figure 2: Behaviour of capture-width ratio: (a) $x_i = \pm[0, L/3, 2L/3, L]$, $D = \bar{D}$; (b) $x_i = \pm L$, $D = \bar{D}$; (c) continuous PTO, $D = \bar{D}$; (d) $x_i = \pm[0, L/3, 2L/3, L]$, $D_m = \bar{D} \times [0.1, 1, 10]$; (e) $x_i = \pm[0, L/3, 2L/3, L]$, $D_m = \bar{D} \times [10, 1, 0.1]$; and (f) continuous PTO, $D_m = \bar{D} \times [10, 1, 0.1]$.

3 Results

In this section we examine the effects of plate flexural rigidity, PTO and wave frequency on C_W. For simplicity, let us consider a water-plate system with the following fixed parameters: $A = 1$ m, $h = 10$ m, $L = 20$ m, $k_{PTO} = 0$ and $\rho = 1000$ kg m^{-3}. Herein, we select $j = 20$ evanescent modes and consider the first $l = 12$ dry elastic modes, whereas the Fourier sine series is truncated at $n = 100$. Figure 2(a)-2(b) show the surface plot of the capture-width ratio C_W as a function of incident wave frequency and PTO coefficient for flexural rigidity $D = \bar{D} = 6.9 \times 10^4$ kg m^3 s^{-2}, $\mu = 44$ kg/m and two different PTO distributions, i.e. seven equally spaced PTO devices located across the plate and two PTO devices located at the plate edges, respectively. We note that as the number of PTOs increases, the system becomes more efficient. Figure 2(c) presents results for the idealised case of a continuous system of PTO cables ($\mathcal{I} \to \infty$), simulating the effect of a great number of discrete devices beneath the plate. Several peaks of magnitude $C_W \sim 1$ can be discerned, hence, plate elasticity acts to further increase power extraction. We now investigate the effect of flexural rigidity distribution D on power extraction efficiency. For simplicity, we consider a plate made of $M = 3$ segments each of length $2L/3$ and constant D_m, $m = 1, 2, 3$. Figure 2(d) concerns a case where the plate flexural rigidity increases towards the plate front, such that $D_m = \bar{D} \times [0.1, 1, 10]$. The efficiency is rather poor because the plate enhances wave radiation as $x \to -\infty$. Figure 2(e) shows the map obtained for D increasing towards $x = -L$ such that $D_m = \bar{D} \times [10, 1, 0.1]$. This case achieves much greater efficiency, with the map also containing several additional peaks at high frequencies. Figure 2(f) presents C_W maps for continuous PTO system and rigidity increasing towards $x = -L$, $D_m = \bar{D} \times [10, 1, 0.1]$. This case attains high efficiency over a rather large frequency bandwidth, and is the best configuration analysed herein from an energy extraction efficiency perspective.

Acknowledgement: The authors acknowledge support from the University of Plymouth Centre for Decarbonisation and Offshore Renewable Energy (CDORE) Seedcorn Funding.

References

Newman, J. N. (1994), 'Wave effects on deformable bodies', *Appl. Ocean Res.* **16**, 47–59.